

EFFECT OF CONDUCTING PLATES ON COHERENT SPACE CHARGE PHENOMENA

A. G. RUGGIERO, P. STROLIN, V. G. VACCARO

CERN, Geneva, Switzerland

Presented by E. Keil

1. Introduction

The dispersion relations between the mode number n and the frequency ω of longitudinal and transverse perturbations of a coasting beam are ^{1,2}

$$-1 = (U - iV)_l \int \frac{f'(w)dw}{\omega - n\Omega} \quad \text{and} \quad 1 = (U + iV)_t \int \frac{g'(a)a^2 da}{(\omega - n\Omega)^2 - Q^2\Omega^2} f(w)dw \quad (1)$$

The functions $f(w)$ and $g(a)$ are the particle distributions functions in angular momentum and betatron amplitude. The quantities U and V are related to the e. m. fields induced by the beam perturbation in the surrounding medium, and scattered back on the beam, and can be in general represented by impedances loaded by the beam perturbation, as for example shown in ref. (3). The solution of the dispersion relation is now understood ¹⁻⁶ so that the thresholds of (U, V) are found. They depend only on the phase space and optical parameters of the beam. The complementary step consists in expressing (U, V) in terms of the machine equipment parameters. The diversity of the components that are likely to interact with the beam ^{1-3,7-9} may lead to a variety of difficulties.

Experiments at the MURA 50 MeV FFAG Accelerator ¹⁰ produced evidence for coherent transverse instabilities caused by clearing field plates. Following these experiments, Laslett⁸ studied the effect of a centrally loaded plate for the transverse case, assuming the charge and the current distribution on the plate to be governed by transmission line equations. Recent observations on Adone ¹¹ show a clear connection between the thresholds of transverse instability and the presence of electrodes near the tank wall.

In this paper we give a concise presentation of the basic results obtained in a recent theoretical study⁹. These results are then interpreted by means of the familiar concepts of lumped circuits, using the appropriate e. m. models.

2. Basic results

In the long wavelength limit the plate does not resonate. Its behaviour is weakly capacitive if unloaded, strongly inductive if short-circuited^{3, 8, 9}. In other words, the plate is more or less strongly coupled to the beam depending on the load. We have the same behaviour in the short wavelength range. At resonance short-circuited plates are strongly coupled to the beam, unloaded plates are weakly coupled. We point out that in both these extreme cases the high Q of the resonance is determined by the dissipation on the plate. The intermediate behaviour is modified by the fact that the resonance can be damped by the dissipation on the terminating impedance.

We consider the cylindrical geometry shown in Fig. 1. The charge density is uniform within the beam cross-section. Using the transmission line model⁸, we get the additional (U, V)-factors for longitudinal and transverse motion due to the presence of M identical plates of characteristic impedance $Z_0 = (L/C)^{1/2}$

$$\begin{aligned} \frac{(U_1 - iV_1)_l}{nm_0c^2} &= \frac{4\pi}{\beta_p} \left(\frac{Z_0 l}{E_0/e} \right) \left(\frac{Ml}{2\pi R} \right) K_1^2 P(\omega, n), \\ \frac{(U_1 + iV_1)_t}{\omega_0} &= - \left(\frac{4}{Q\gamma_p \beta_p^3} \right) \left(\frac{Z_0 l}{E_0/e} \right) \left(\frac{Ml}{2\pi R} \right) \left(\frac{R}{b} \right)^2 K_1^2 P(\omega, n), \end{aligned} \quad (2)$$

where $\beta_p = \omega_0 R/c$ is the particle velocity, $\gamma_p^{-2} = (1 - \beta_p^2)$, E_0 the particle rest energy and I the beam current. The K-factors⁹ take into account the aperture ϕ_0 of the plate, whereas the P-factor describes the electrical response of the device.

The electrical response of a perfectly conducting plate loaded with an impedance $Z_r = rZ_0$ at a distance d from the edge is:

$$P = 2\beta_w(\beta_w - \beta)(1 - \beta_w\beta) \frac{\cos\Phi(1 + \delta)\sin\theta(1 - \delta) + \cos\Phi(1 - \delta)\sin\theta(1 + \delta)}{(1 - \beta_w^2)^2(\cos 2\delta\Phi + \cos 2\Phi - 2ir\sin 2\Phi)\theta} - \beta_w \frac{\sin 2\Phi[(1 - \beta_w\beta)^2 + (\beta - \beta_w)^2] + 2ir(1 - \beta_w\beta)^2(\cos 2\Phi - \cos 2\theta)}{(1 - \beta_w^2)^2(\cos 2\delta\Phi + \cos 2\Phi - 2ir\sin 2\Phi)\theta} \frac{(\beta_w - \beta)^2}{1 - \beta_w^2} \quad (3)$$

where $(\beta = \beta_w$ for long. case, $\beta = \beta_p$ for trans. case)
 $\theta = \frac{n l}{2R}$; $\Phi = \frac{\omega l}{2c} = \beta_w \theta$; $\delta = (1 - 2d)/l$; $r = r' - ix'$

From refs. (1), (2) we get

$$\beta_w \approx \beta_p \quad \text{and} \quad \beta_w \approx (1 - Q/n)$$

for the longitudinal and transverse case, respectively.

3. Discussion and practical implications

In the long wavelength limit Eq. (3) gives:

$$P = \frac{1 \cdot (-2ir\Phi)}{1 - 2ir\Phi} - \beta^2 \quad (\Phi \ll 1) \quad (4)$$

As pointed out in³ the form (4) is the response of the distributed circuit of Fig. 2a, which corresponds to the concentrated circuit Fig. 2b, where the normalized impedances $-\beta^2$ and 1 take into account the inductance and the capacitance of the plate, respectively. For almost floating plates ($|r\Phi| \gg 1$)

$$P = (1 - \beta^2) - 1/2r\Phi \quad (\Phi \ll 1) \quad (5a)$$

which indicates, for $\gamma_p \gg 1$, a strong cancellation between the e. m. forces. This result is illustrated by the configuration of e. m. fields given in Fig. 2c, where the arrows indicate the electric field (i. e. the capacitive term 1) and the crosses the magnetic field (i. e. the inductive term $-\beta^2$). For almost short circuited plates ($|r\Phi| \ll 1$)

$$P = -\beta^2 - i2r\Phi \quad (\Phi \ll 1), \quad (5b)$$

which shows that there is no longer any cancellation in the region between the plate and the wall, as illustrated in Fig. 2d. The electric field lines are shunted by the terminating impedance and there is left only the inductive term $-\beta^2$ and a small term depending on the termination. For drift tubes ($\varphi_0 = \pi$) placed inside a pipe of radius b' and extending over the whole circumference, we get^{3,9} for the longitudinal case $K_1^2 = 1/2$, $C = [2\ln(b'/b)]^{-1}$, and therefore

$$U_1 = \frac{2Ne^2}{R} (1 - \beta_w^2) \ln \frac{b'}{b} \quad (\Phi \ll 1). \quad (6)$$

This form added to the one given in ref. ¹, to get the total U , gives an expression which is nothing but the one for a smooth pipe of radius b' . The total response is still capacitive. On the other hand a few loaded plates can make the total response inductive; for this it is sufficient, from Eq. (3.9a) of ref. ¹ and Eq. (5b) that

$$(1 - \beta_w^2) \left(1 + 2 \ln \frac{b}{a}\right) < \left(\frac{Ml}{2\pi R}\right) \beta_w^2 \ln \frac{b'}{b} \quad (\Phi \ll 1) \quad (7)$$

Similar considerations apply to the transverse case.

For what concerns the resonant behaviour of the device, it is apparent from its electrical configuration that the response is that of a parallel circuit. Then the resonance occurs when the reactance of the transmission line cancels the reactance of the termination, i. e.

$$\frac{1}{X_T} = \frac{\text{tg}\Phi(1+\delta)}{Z_0} + \frac{\text{tg}\Phi(1-\delta)}{Z_0} \quad (8)$$

In fact we see from Eq. (5) that the P-factor has its maximum when

$$\cos 2\delta\Phi + \cos 2\Phi - 2x' \sin 2\Phi = 0, \quad (9)$$

which is nothing but Eq. (8) expressed in a different form. As for a parallel RLC circuit, where the impedance at resonance is $(L/C)/R$, in this case we find at these loaded resonances

$$V_1 \sim Z_0 P = Z_0^2 / (2\theta R_T). \quad (10)$$

For $R_T \rightarrow 0$ the resonance is damped by the dissipation on the plate. To work out the P-factors, the transmission line equation must be modified taking into account the surface resistivity⁹. In this case we get at resonance for $\delta' = 0$

$$V_1 \sim Z_0 P = Z_0^2 / (\theta R_p), \quad (11)$$

where R_p is the resistance of the plate due to the skin effect.

When the condition

$$\sin 2\Phi = 0, \text{ i. e. } \Phi = \pi\nu/2 \quad (\nu \text{ pos. int.}) \quad (12)$$

is satisfied, floating plates resonate. Also in this case the figure of quality is high since the dissipation takes place only on the plate. However, like in the long wavelength limit, unloaded plates are weakly coupled to the beam. This seems to be due to the partial cancellation of the potential wave induced on the plates by the waves reflected at its ends. The unloaded resonance response is⁹:

$$V_1 \sim Z_0 P \approx \gamma_p^{-2} Z_0^2 / (\theta R_p) \quad (13)$$

Unloaded resonances can also occur for loaded plates when the terminating impedance is at a node of the voltage standing wave pattern at resonance. This occurs when in addition to Eq. (9) also Eq. (12) is satisfied, which implies:

$$|\delta'| = (\nu + 1 - 2p) / \nu \quad (p \text{ pos. int. } < (\nu + 1) / 2). \quad (14)$$

The lowest of the above resonances goes to infinity when $|\delta'| \rightarrow 1$, hence unloaded resonances for loaded plates disappear when the terminating impedance is at one of the ends of the plate. This corresponds to the physical fact that the end of the plate cannot be a maximum of the potential (resonant plate) and at the same time a node (unloaded resonant plate).

We have seen that the unloaded plates present a weaker coupling to the beam perturbation than loaded plates and that in general the resonant response is proportional to the square of the characteristic impedance. One should then have a large terminating impedance and a small characteristic impedance. The first condition usually conflicts with the function of the plates (clearing field electrodes), which have to be fed by a high voltage supply via a coaxial line. In fact, for certain frequencies the plate would see a very low impedance, which is the trans-

formation of the very high one of the supply since the cable is mismatched. One then has the short circuited plate response which is the worst condition found. The internal impedance of the supply has to be shunted with a resistor matched to the transmission line, in order to have a constant impedance at the plate.

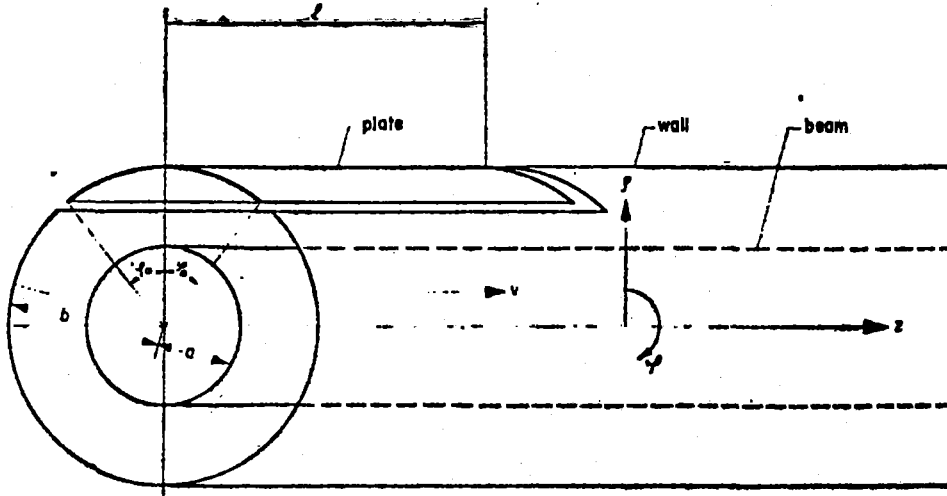


Fig. 1 Geometrical configuration of the pipe and of the plate.

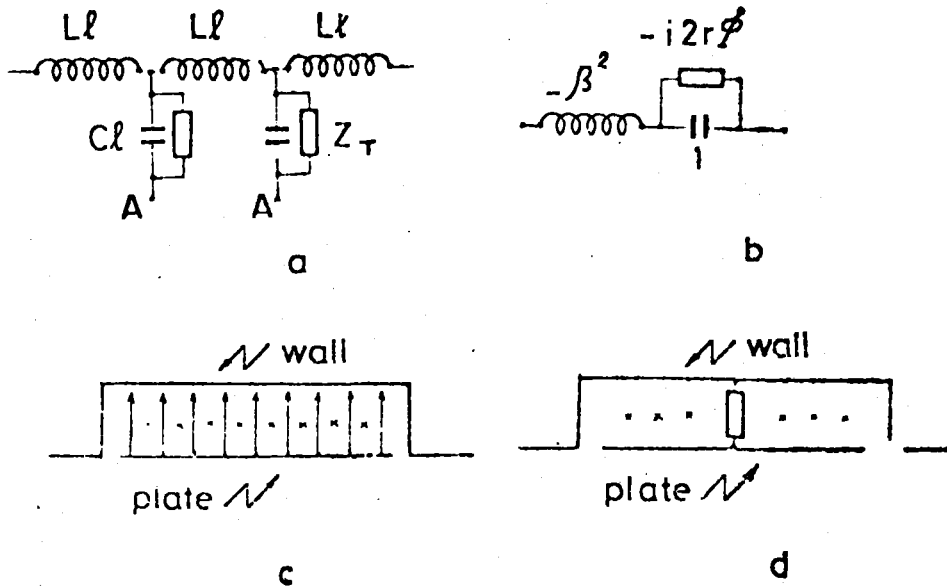


Fig. 2 a) Distributed circuit representing a series of plates. Points A, A are the surface of the plate collecting the charges induced on the wall and loaded by the transverse perturbed current.

b) Lumped circuit equivalent to the distributed one loaded by the longitudinal perturbed current.

c), d) Electromagnetic configuration inside the space between the plate and the wall. The cancellation effect $(1-\beta^2)$ takes place for unloaded plates (Fig. 2c). The capacitive effects are shunted and suppressed by the terminating impedance (Fig. 2d). No cancellation effect any more $(-\beta^2)$.

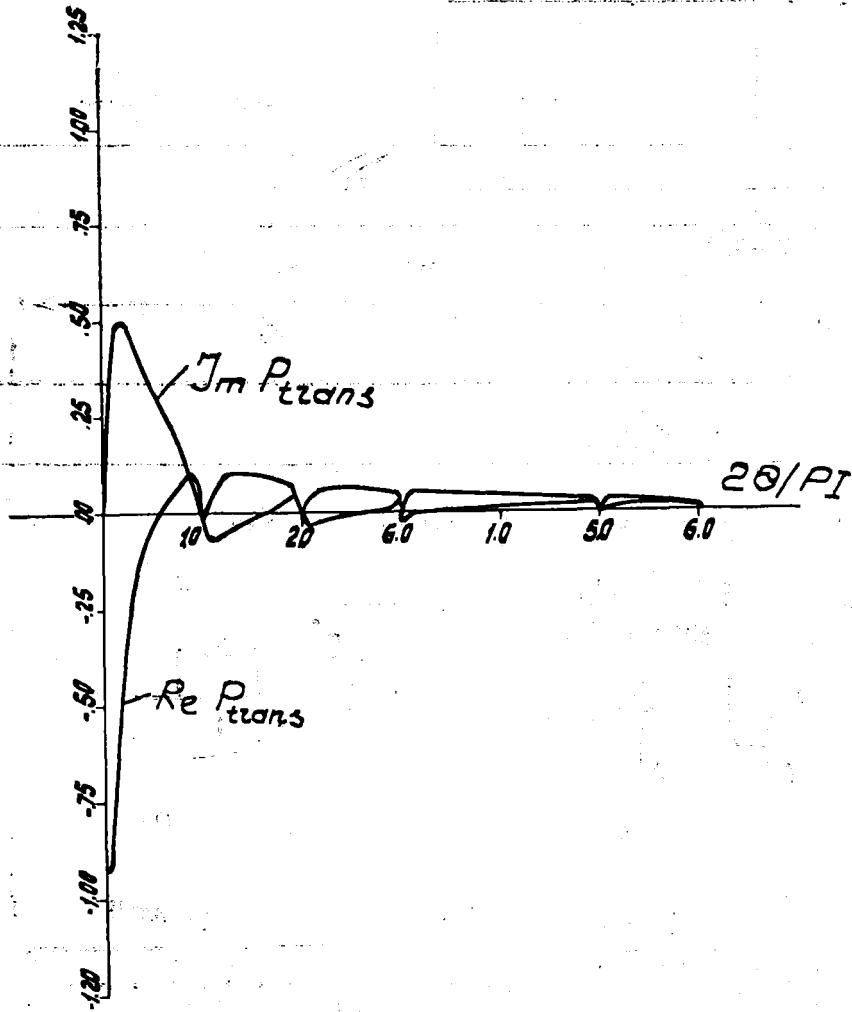


Fig. 3 Typical behaviour of the P-factor in the transverse case as a function of $2\theta = (n\lambda)/R$, for $(1/R) = 1.67 \times 10^{-3}$ and $Q = 8.75$ (ISR clearing field electrodes). Loaded resonances appear as broad-band resonances [$\theta \approx \pi(2k-1)/2(1 \pm b)$]. An unloaded resonance appears at $\theta \approx 2\pi$ [in general when $(2k-1)/(1 \pm b)$ equals a positive integer] as a narrow spike. This can appear on the plot due to the rather low value of γ_p . For the longitudinal case we have a quite similar behaviour, because of the very small value of $1/R$.

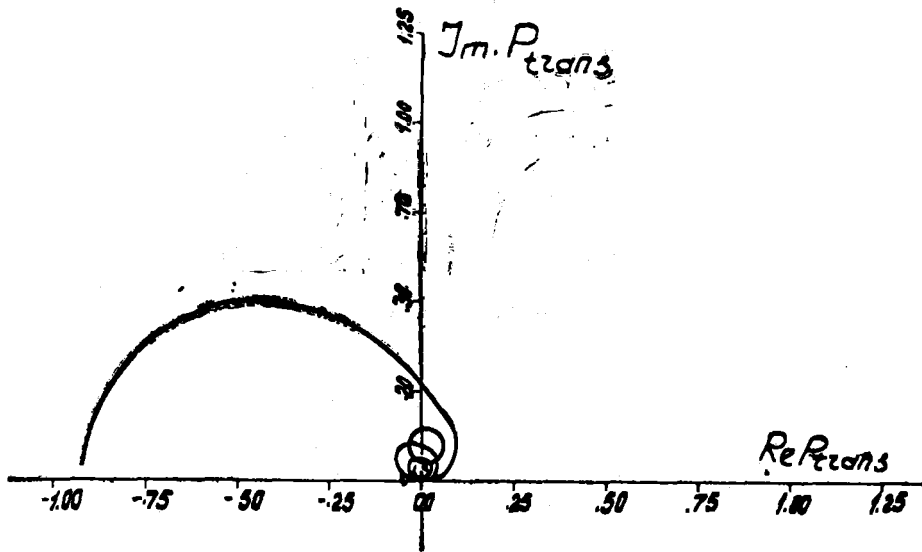
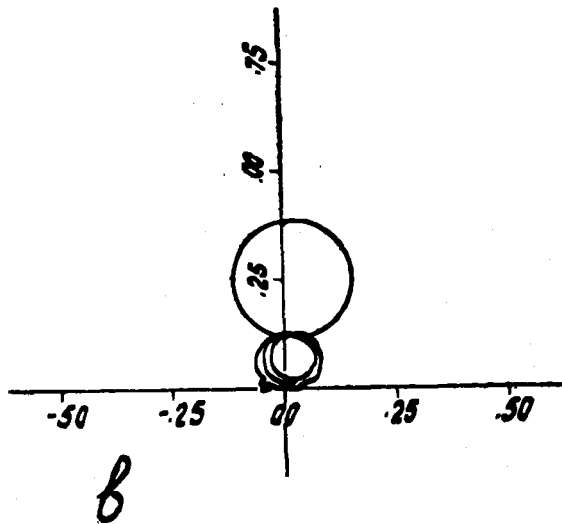


Fig. 4_a) The transverse P-factor in the complex P-plane, with θ as a running parameter. The loaded resonances appear as a spiral tangent to the real axis. Unloaded resonances ($\theta \approx 2\pi$) appear as a perfect circle tangent to the curve of loaded resonances. The resonant behaviour is complicated by the factor $\theta - 1$ which appears in equation (3)



b) In Fig. (4b) we have $P\theta/2$, which allows one to visualize better the loaded resonance response (rough circles tangential to the real axis). However, the use of P as in Fig. (4a), allows direct insertion into stability diagrams.

REFERENCES

1. **V. K. Neil and A. M. Sessler**, *Rev. Sci. Instr.* **36**, 429, 1965.
2. **L. J. Laslett, V. K. Neil and A. M. Sessler**, *Rev. Sci. Instr.* **36**, 436, 1965
3. **A. M. Sessler and V. G. Vaccaro**, CERN 67-2, 1967.
4. **R. L. Pease**, *IRE Trans. on Nucl. Sci.* **12**, 561, 1965.
5. **A. G. Ruggiero and V. G. Vaccaro**, CERN Int. Report, ISR-TH/68-33, 1968
6. **A. G. Ruggiero, K. Hübner and V. G. Vaccaro**, paper presented at this conference.
7. **R. J. Briggs and V. K. Neil**, UCRL-14407-T, 1965.
8. **L. J. Laslett**, *Proc. Int. Symp. Ekt. Posit. Storage Rings, Saclay* (1966).
9. **A. G. Ruggiero, P. Strolin and V. G. Vaccaro**, CERN Int. Report, ISR-RF-TH/69-7, 1969.
10. **C. Curtis et al.**, *Proc. Int. Conf. High En. Acc. Dubna, 1963, Atomizdat, Moscow, 1964.*
11. **F. Amman et al.**, *Lettere al Nuovo Cimento*, **1**, 729, 1969.